THE DYNAMIC IMPACT STUDY OF A CRANK CONNECTING ROD MECHANISM

Andra CONSTANTIN, Oana OȚĂT, Adrian CALANGIU, Nicolae CRĂCIUNOIU, Alexandru MARGINE, Nicolae DUMITRU

Abstract: *The mechanical impact phenomenon emerges in fast-moving mechanical systems when some of the moving elements reach critical positions.*
The first section of the present paper is concerned with the dynamics of the impact between a freely moving bar and a fixed plate.
In the second section, we set out to investigate the impact phenomenon's effect on the dynamic response of an actuation mechanism on an internal combustion engine. Our research study addressed a crank connecting rod mechanism to which we considered a radial clearance in the joint that links the connecting rod to the piston. Under these conditions, during the operation of the mechanism develops an impact that influences the kinematic parameters that define the movement of the two bodies in contact.
Key words: *dynamic, impact, engine torque, finite element, rigidity, damping.*

1. INTRODUCTION

An expression for permanent deformation, resulting from the impact of a bar with a flat surface can be found in [1].

The analysis of the bar movement was made by shooting with an ultrafast camera with about 1000 frames per second. Mathematical models have been studied for the elastic phase and the elasto-plastic phase. The two phases are based on the Hertzian theory approached according to the Jackson Green Model.

In what follows we have developed five different models: The Jackson Green model, the Kogut-Komvopoulos model, the Thornton and Ning model, the KE model and the case-study model developed in the present paper. Each model implies a loading and unloading phase.

The model presented in the paper includes the deformation effect on the bar and the support surface and highlights a novel expression for the permanent deformation resulting from the impact between the two objects.

Of note is the work [2], where a mathematical model is developed that aims at establish the connection between the impact duration, the permanent normal deformation and the slip length.

We analysed these elements in the case of the impact between a bar and a flat surface. The sliding length in our case is the slider-distance. Velocities before and after impact have been experimentally established, as have permanent deformations after impact. The experimental results coincide with the numerical simulations only for the normal impact, while for the oblique impact the results are different.

Paper [3] introduces some aspects regarding the modelling and simulation of mechanical systems in which contact-impact problems occur.

We have adopted the Theory of Multibody systems (Newton-Euler approach) and considered the bodies in the structure as rigid. Several contact models are analyzed, i.e. pure elastic contact force models, and dissipative contact force models. Based on the above-mentioned models, we framed the main

characteristics, advantages and limitations of the contact force models presented above were analyzed.

The dynamic response of a connecting rod-crank mechanism, considering a move in the joint that links the connecting rod and the slider (connecting rod and the slider) is analyzet by Olya A.A, and Ghazavi M. R. [4].

The movement frequency leads to loss of contact and chaotic behavior of the system. The mechanism control is based on the Piragas method, Accordingly, a proper control prevents the loss of contact whereas the mechanism displays a periodic movement by applying small perturbations.

Elements of mathematical modeling and virtual prototyping on the impact phenomenon in case of two bodies, with a fixed one and another on in free motion are presented in [5]. In this case, the impact force is identified by means of mathematical models and analysis via the finite element method.

A formulation for the analysis of impact-related problems with friction in the case of multibody mechanical systems, can be found in [6]. This formulation is based on a canonical form of the equations of motion using joint coordinates and joint momenta.

We aim at investigating the impact between two bodies, within the structure of a mobile mechanical system of a crank-connecting-rod type. In fact, the actuation mechanism of a compressor engine. The conditions for the occurrence of an impact force during the operation of the mechanism envisage execution and assembly errors that lead to a radial clearance between the connecting rod and the piston pin. This radial clearance has the value of 0.03 mm. During the operation of the mechanism rapid movements develop, materialized by relatively high speeds and accelerations.

The impact problem between the components of this type of mechanism has been studied for different pairs of materials. The paper brings forward the results for two such pairs, i.e. steel-aluminum and steel-cast iron. These pairs refer to the materials from which the bearing mounted

in the small head of the connecting rod and respectively the piston bolt are made.

The coefficient of rigidity K, depends on the material and the radii of the solid bodies in contact.

2. MATHEMATICAL MODELS

To study the dynamic response of the mechanism under the given conditions, we resorted to the dynamic module of the Adams software.

We set out to analyse the behavior of the mechanism in two situations, i.e. when the kinematic elements are rigid and then when they are deformable.

Geometric errors due to the clearance in the joints lead to jumps in the variation of kinematic parameters and implicitly to the appearance of impact forces.
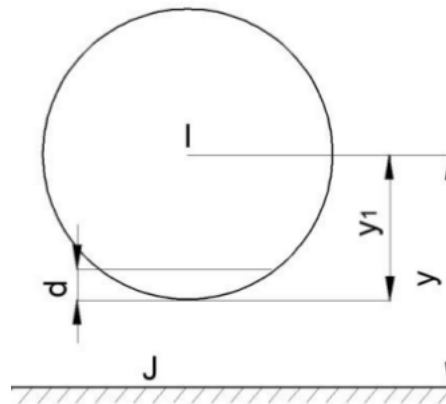

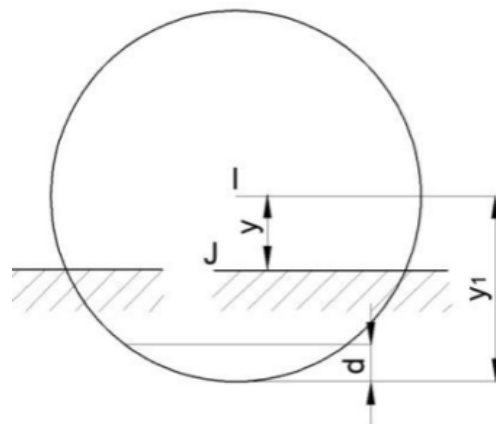**Fig. 1.** Spherical-planar contact type (before contact)

Fig. 2. Spherical-planar contact type (after contact)

To model the impact phenomena developed in the Adams software, we relied on the following mathematical model:

$$F_{impact} = F\left(y, \dot{y}, y_1, k, e, c_{max}, d\right) \quad (1)$$

Where:

y -distance depending on time, which is necessary for the impact function calculus, namely: $y_A = y_A(t)$;

$\dot{y} = \dfrac{dy}{dt}$ -the point speed at which it will consider that it will actuate the impact force, i.e., speed $\dot{y} = v_A$ (point A speed);

y_1 -a positive real variable, which can be considered to be the free length of y component displacement;

k -stiffness which corresponds to the interaction between the bar and the contact surface;

e -is a positive real variable which specifies the deformation characteristics exponent of the applied force;

c_{max} -is a non-negative, double-precision variable that specifies the maximum damping coefficient;

d -is a positive double-precision variable that specifies the secondary penetration at which ADAMS/Solver applies full damping.

To establish rigidity, we applied the following expression:

$$K = \frac{4}{3\pi\left(h_i + h_j\right)} R^{1/2} \quad (2)$$

$$R = \frac{R_i R_j}{R_i + R_j} \quad (3)$$

$$h_k = \frac{1-\nu_k^2}{\pi E_k}, k = i, j \quad (4)$$

Where:

R_i -represent the radius of the i-body in contact;

ν_i - represent the Poisson coefficient;

E_i -represent the longitudinal elasticity module for the i-body.

R_j -represent the radius of the j-body in contact;

ν_j -represent the Poisson coefficient;

E_j -represent the longitudinal elasticity module for the j-body.

The impact force was determined for two couples of materials.

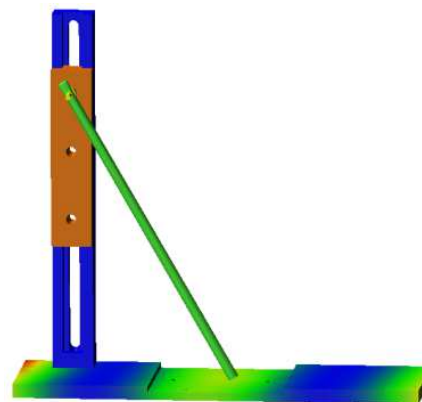## 2.1 Dynamic model of the impact between the bar and the flat board.

Fig. 3. Bar-flat board geometric model

In a first stage, we study the dynamics of the impact for a simple plane kinematic chain composed of a bar that moves freely under the action of the gravitational force and a flat board.

The dynamic model of the impact force is of the type indicated in the relation (1):

IMPACT (. MODEL_2. dz_42,. MODEL_2. vz_42, 1.0 E-02, 250000, 2, 10, 0.1)

Where:

-dz_42 is the Z-axis displacement of the marker 42;

-vz_42 is the Z-axis velocity of marker 42;

-distance y_1=1.0 E-02;

-rigidity k=250000;

-force coefficient e=2;

-damping factor c_{max}=10;

-penetration depth d=0.1.

To monitor the transverse elastic displacements of the flat board, the flat board body was transformed from a rigid to a flexible body, by applying the finite element method.

The dynamic impact study was performed for two situations, when the force coefficient is 2.2 (Figure 8) and 1.95 (Figure 9) respectively.

Monitoring the dynamics of the impact phenomenon was carried out for several pairs of materials. The paper focuses on the pairs of materials when the bar and the flat board are made of steel.
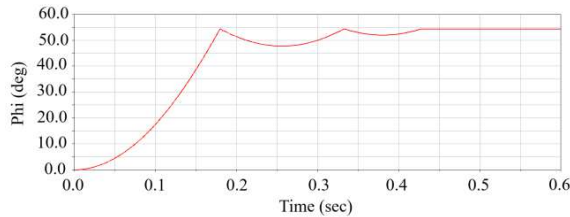

Fig. 4. Variation of the rotation angle of the bar

In Figure 4, we indicate the variation diagram of the angle in the rotation coupling, in relation to the local axis system centered in this coupling (Z axis). According to the diagram, we can identify the moments of time when the contact between the bar and the flat board occurs, including the duration of the contact.
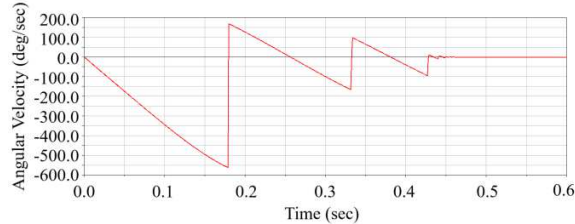

Fig. 5. Variation in the angular velocity of the bar

Figure 5 shows the variation diagram of the angular velocity of the bar.

The variation is influenced by the impact between the bar and the flat board. It is obvious that the jumps in the diagram are influenced in form, frequency and value, mainly by the damping coefficient.
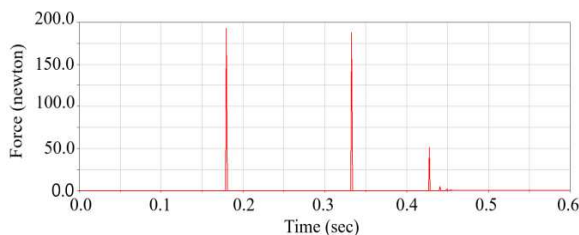

Fig. 6. Impact force variation diagram

The impact force variation diagram in Figure 6 shows the amplitude and frequency of the contact.

As recorded, the amplitude of the force decreases after the first contact, and in the end, it is damped. The frequency of the contacts generated by the impact between the bar and the flat board highlights the idea that the impact force actually has two components, namely an elastic one, influenced by the rigidity of the bodies in contact, and, a viscous one, influenced by the speed of the bar movement and the damping coefficient.
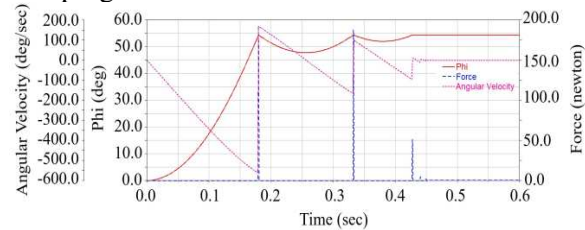

Fig. 7. Variation of kinematic and dynamic parameters

In Figure 7 we have superimposed the time variation curves for the impact force, the rotation angle and the angular velocity.

The aim was to monitor the synchronization of the parameter jumps relative to the moments of time when the contact between the bar and the flat board is repeated. As indicated in the figure, this timing is perfect.
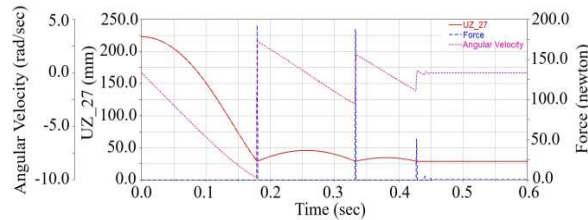

Fig. 8. Variation curves for impact-model 1

IMPACT (.MODEL_2. DZ_27,.MODEL_2. VZ_27,29, 307692,2.2,0.08,0.01)
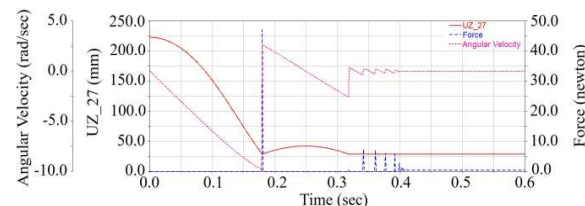

Fig. 9. Variation curves for impact-model 2

IMPACT (.MODEL_2. DZ_27,.MODEL_2. VZ_27,29, 307692,1.95,0.08,0.01)

Figure 8 and 9 display the time variation curves for the displacement of the marker 27 (the point of application of the impact force), the impact force and angular velocity of the moving bar.

We note that the impact force harmonics are larger than the amplitude in Model 1 and smaller in Model 2.

At the same time we record an almost perfect correspondence between the jumps of the impact force, respectively of the angular velocity and respectively of the displacement of the bar (UZ_27).
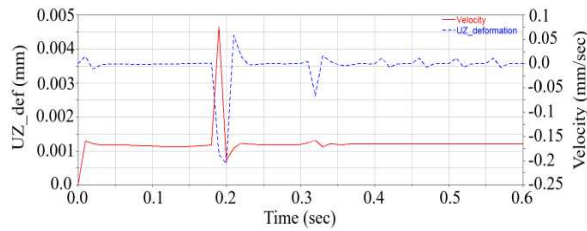

Fig. 10. Variation of kinematic parameters of the flat board

Figure 10 shows the time variation curves for the elastic transverse displacement of the flat board and correspondingly for the speed in the movement of the plate as a deformable body. In this case as well, the temporal correspondence between displacement and velocity is recorded at the moments of time generated by the harmonics of the impact force.

In the processing of the dynamic models, special importance is paid to the adopted integration method and the integration step.

2.2 The steel-aluminium materials pair (piston bolt-steel; connecting rod bearing aluminium).

The module of elasticity for steel: $E_1 = 210000 MPa$;

Elasticity module for aluminium: $E_2 = 71000 MPa$;

Coefficient of transverse contraction: $\nu_1 = 0.3$;

Coefficient of transverse contraction: $\nu_2 = 0.33$

$$h_1 = \frac{1-\nu_1^2}{\pi E_1} = \frac{1-0.3^2}{\pi \cdot 210000} = 1.3793 \cdot 10^{-6} \tag{5}$$

$$h_2 = \frac{1-\nu_2^2}{\pi E_2} = \frac{1-0.33^2}{\pi \cdot 71000} = 3.9951 \cdot 10^{-6} \tag{6}$$

$$R = \frac{R_1 R_2}{R_1 + R_2} = \frac{20 \cdot 20.02}{20 + 20.02} = 10.0049975012 \tag{7}$$

$$K = \frac{4}{3\pi (h_1 + h_2)} R^{1/2} = 249804.08223 \tag{8}$$

We developed the virtual prototyping of the mechanism, considering the kinematic elements, inertial properties and the clearance mentioned above.

The dynamic model of the impact force was designed based on the kinematic and dynamic parameters presented in the relation (1).

The application point of the impact force is marker 42, the centre of rotation of the piston bolt (spindle-bearing joint), Figure 11 and 12.
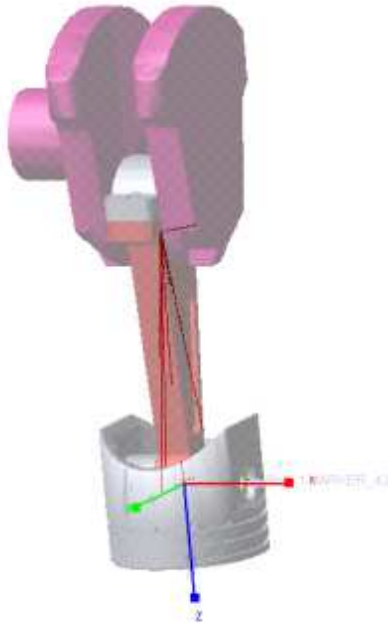

Fig. 11. Geometric model of the mechanism

Fig. 12. The location of marker 42

The transformation of the connecting rod of the mechanism from rigid body to deformable body is based on the finite element method as follows:

- The virtual model of the connecting rod as a rigid body was discretized into finite elements of hexahedral type;

- The connecting rod conditions inside the mechanism were defined by identifying the Master-and-Slave-type nodes;

- A modal analysis of the connecting rod was performed with the determination of natural frequencies and their own vibration modes, necessary for a complete dynamic analysis of the mechanism.

In a first stage, the dynamic study of the mechanism on the model with rigid kinematic elements consisted in identifying the variation law of the torque moment that rotates the crankshaft (slider crank).

The analytical expression of the motor moment is:

$$T_m = T_0 * \left(1 - WZ\left(MARKER\_i, MARKER\_j, MARKER\_k\right) / \omega_0\right) \quad (9)$$

Where:
T_m- motor moment;
T_0- initial moment;

WZ- angular velocity of the crankshaft in operating mode (to MARKER_i, from MARKER_j, about MARKER_k);

ω_0- initial angular velocity.

In the case of the mechanism under investigation, the expression of the torque moment processed in Adams is:

$$T_m = -9E - 8 * \left(1 - WZ\left(MARKER\_1, MARKER\_2, MARKER\_2\right) / 2\right)$$

The impact force built within the Adams environment, based on the relation (1), has the expression:

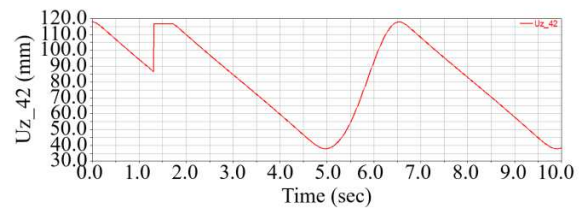IMPACT(MODEL_2.dz_42,.MODEL_2.vz_42, 1.0 E-02, 250000, 2, 10, 0.1)

Fig. 13. Z-axis displacement variation of marker 42

Figure 13 shows the variation of the displacement after the Z-axis of marker 42, the Z-axis being the longitudinal axis of the piston. In essence, this diagram indicates the variation in piston stroke.
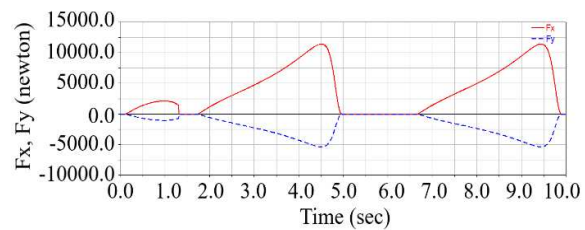

Fig. 14. Variation diagrams of the impact force components by x-axis and y-axis

Figure 14 shows that the impact force component after the x axis registers maximum values up to 12000 [N], and the component after the y axis up to 5000 [N].
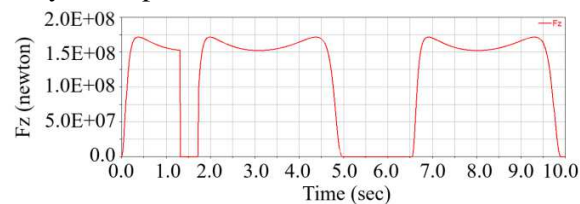

Fig. 15. Variation diagram of the impact force component by z-axis

As indicated in Figure 15, the component after the z axis has maximum values reaching up to 2×10^8 [N].

The diagrams in Figures 14 and 15 show the variation of the components of the impact force before impact, during impact and after impact.

We note that the jumps in the variation of these forces correspond to the moment of time in which the two bodies come into contact.
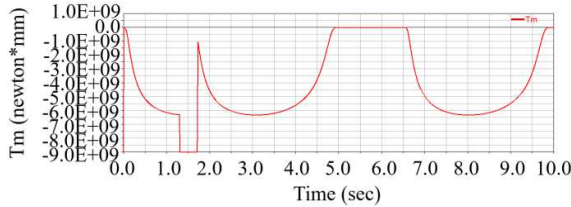

Fig. 16. Engine torque variation diagram

The torque moment variation diagram in Figure 16 records a jump at start due to inertia and the presence of the impact force. The mode of variation is similar to that of the kinematic parameters and the impact force during the operation of the mechanism.
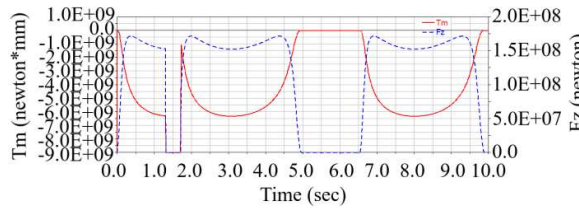

Fig. 17. Variation diagrams for the impact force and the engine torque
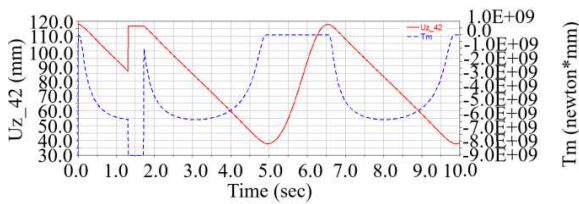

Fig. 18. Variation diagrams for the engine torque and exceeding the marker 42

The mode of variation of the dynamic components respectively the engine torque and the impact force is shown in Figure 17.

We note that the two components have maximum values during the contact between the two bodies so that the oscillations of the engine torque are influenced by the mode of variation of the impact force.
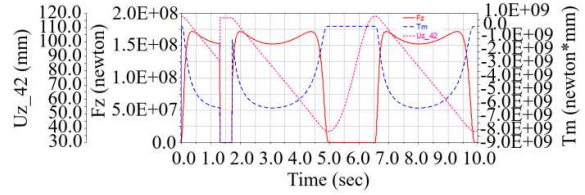

Fig. 19. Variation diagrams for Tm engine torque, Fz impact force and marker 42 displacement

Figure 19 illustrates superimposed variation diagrams for piston displacement, impact force Fz and engine torque T_m.

Accordingly, the impact between the two bodies generates several moments of contact over a 10-second interval.

2.2 The steel-aluminium materials pair (piston bolt-steel; connecting rod bearing aluminium).

Module of elasticity for steel: $E_1 = 210000 MPa$;

Modue of elasticity for cast iron: $E_2 = 1.1 \cdot 10^5 MPa$;

Coefficient of transverse contraction: $\nu_1 = 0.3$

Coefficient of transverse contraction: $\nu_2 = 0.28$.

$$h_1 = \frac{1 - \nu_1^2}{\pi E_1} = \frac{1 - 0.3^2}{\pi \cdot 210000} = 1.3793 \cdot 10^{-6} \quad (10)$$

$$h_2 = \frac{1 - \nu_2^2}{\pi E_2} = \frac{1 - 0.28^2}{\pi \cdot 1.1 \cdot 10^5} = 2.668 \cdot 10^{-6} \quad (11)$$

$$R = \frac{R_1 R_2}{R_1 + R_2} = \frac{20 \cdot 20.02}{20 + 20.02} = 10.0049975012 \quad (12)$$

$$K = \frac{4}{3\pi (h_1 + h_2)} R^{1/2} = 331781.0413 \quad (13)$$

For the steel-cast iron materials pair, the impact force designed within the Adams software, based on the relation (1), has the expression:

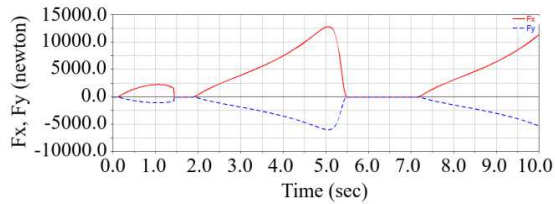IMPACT(MODEL_2.dz_42,.MODEL_2.vz_42, 1.0 E-02, 331781, 2, 10, 0.1)

Fig. 20. Variation diagrams of the impact force
components by x-axis and y-axis

As indicated in Figure 20, in this case the
components of the impact force after the x and y
axes register lower maximum values than those
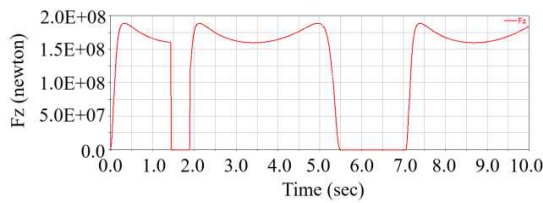shown in Figure 14.

Fig. 21. Variation diagram of the impact force
component by z-axis

According to Figure 21, in this case the
impact force component after the Z axis registers

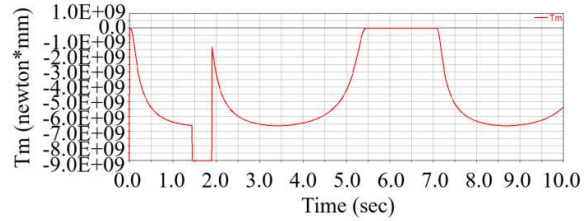a maximum value higher than that shown in
Figure 15.

Fig. 22. Engine torque variation diagram

As recorded in Figure 22, the engine torque
registers the same extreme values as in the
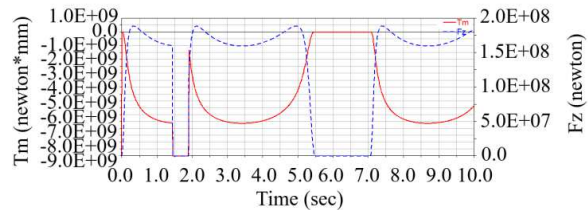previous case, but the variation mode is different
on time intervals.

Fig. 23. Variation diagrams for the impact force and the
engine torque
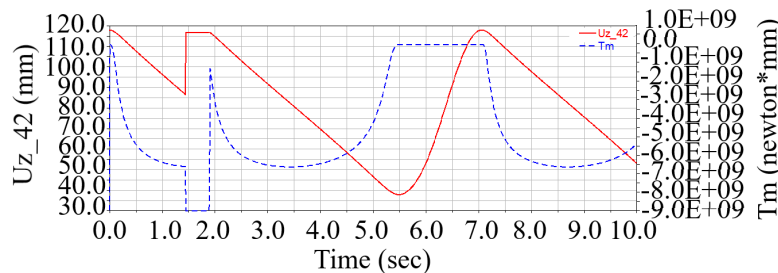
Fig. 24. Variation diagrams for the engine torque and exceeding the marker 42

Fig. 25. Variation diagrams for T_m engine torque, F_z impact force and marker 42 displacement

As in the previous case, the variation
diagrams for the three parameters respectively
piston displacement, impact force and engine

moment were displayed over an interval of 10
seconds, coupled (Figures 23 and 24) and
represented at the same scale as in Figure 25.

We could record that in this case, the contacts

between the two rigid bodies generated by the impact force are in a smaller number than in the first case.
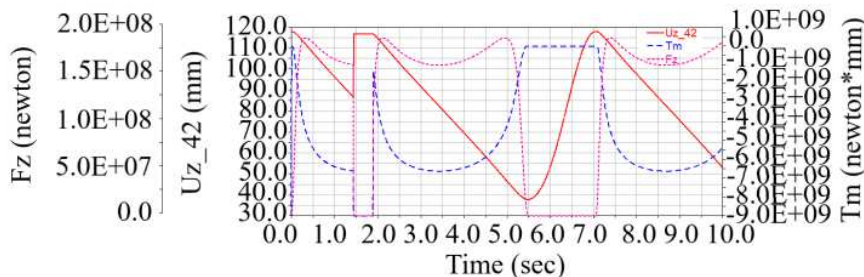
3. CONCLUSIONS

We have analysed the impact force influence in the case of a connecting rod-crank mechanism, with rapid movements, where between the piston bolt and the connecting rod bearing there is a radial clearance of 0.03 mm.

Compared to other research studies, in this case the dynamic response of the mechanism was approached as follows:

-a function was developed within the Adams software, which allows to identify the law of variation of the engine torque (the moment acting on the crankshaft;

-the function of the impact force was developed and the law of variation of the impact force was determined for two pairs of materials: steel-aluminum and steel-cast iron;

-the connecting rod of the mechanism was designed as a deformable body, applying the finite element method, thus the contact under investigation was of the rigid body-deformable body type.

For both situations investigated, we found that the maximum values and the way of variation of the impact force are influenced by the deformability of the connecting rod and, admittedly, by the nature of the materials in contact.

We reached the conclusion that the results of the numerical simulation, particularly the impact force and the engine torque are compatible with the cyclic operation of the mechanism where the deformability of the elements is also taken into account.

We recorded variations in kinematic parameters, especially in the connecting rod -

piston contact area, by monitoring the movement of nodes on the finite elements in the joint.

If the elements are rigid, due to the eccentricity of the spindle-type coupling, the two dynamic components (engine torque and impact force), record jumps in an infinitesimal time at the start of the mechanism.

We consider that these jumps can be neglected and find that the mechanism has a correct cyclic operation, even if in some cases the extreme values of the dynamic components are high. For this reason, a dynamic study of the mechanism is required with the consideration of the elements in contact as deformable.

4. REFERENCES

[1] Ghaednia, H., Marghitu, D. B., and Jackson, R. L., *Predicting the permanent deformation after the impact of a rod with a flat surface,* Journal of Tribology, 137.1, 2015.

[2] Ghaednia, H., & Marghitu, D. B., *Permanent deformation during the oblique impact with friction,* Archive of Applied Mechanics, 86(1), pp. 121-134, 2016.

[3] Machado, M., Moreira, P., Flores, P., & Lankarani, H. M., *Compliant contact force models in multibody dynamics: Evolution of the Hertz contact theory,* Mechanism and machine theory, 53, pp. 99-121, 2012.

[4] Olya, A. A., & Ghazavi, M. R., *Stabilizing slider-crank mechanism with clearance joints,* Mechanism and Machine Theory, 53, pp. 17-29, 2012.

[5] Dumitru, S., Constantin, A., Copilusi, C., & Dumitru, N., *Impact Dynamics Analysis of Mobile Mechanical Systems,* Mathematics, 9(15), 1776, 2021, ISSN/eISSN 2227-7390.

[6] Ahmed, S., Lankarani, H. M., & Pereira, M. F. O. S., *Frictional impact analysis in open-loop multibody mechanical systems*, pp. 119-127, 1999.

[7] Khemili, I., & Romdhane, L., *Dynamic analysis of a flexible slider–crank mechanism with clearance,* European Journal of Mechanics-A/Solids, 27(5), pp. 882-898, 2008.

STUDIUL DINAMIC AL IMPACTULUI LA UN MECANISM BIELĂ MANIVELĂ

Rezumat: Fenomenul de impact mecanic este prezent la sistemele mecanice mobile cu mișcări rapide atunci când unele din elementele în mișcare ajung în poziții critice.
În prima parte a lucrării se studiază dinamica impactului dintre o bară aflată în mișcare liberă și o placă fixă.
În a doua parte se studiază efectul fenomenului de impact asupra răspunsului dinamic al mecanismului de acționare de la un motor cu ardere interna. S-a studiat un mecanism de tip bielă manivelă, la care s-a considerat un joc radial în cupla care face legătura între bielă și piston. În aceste condiții în timpul funcționării mecanismului se dezvoltă un impact ce influențeaza parametrii cinematici care definesc mișcarea celor două corpuri în contact.

Andra CONSTANTIN, PhD student, University of Craiova, Faculty of Mechanics, Calea Bucuresti, street, 107, Craiova, Romania, constantin.raluca.b6c@student.ucv.ro, Office Phone:+40 251 543 739.

Oana OȚÂT, University Lecturer, PhD, University of Craiova, Faculty of Mechanics, Calea Bucuresti, street, 107, Craiova, Romania, otatoana@yahoo.com, Office Phone:+40 251 543 739.

Adrian CALANGIU, PhD student, **Corresponding author**, University of Craiova, Faculty of Mechanics, Calea Bucuresti, street, 107, Craiova, Romania, acalangi@ford.com , Office Phone:+40 251 543 739.

Nicolae CRĂCIUNOIU, Associate Professor, PhD, University of Craiova, Faculty of Mechanics, Calea Bucuresti, street, 107, Craiova, Romania, ncraciunoiu@yahoo.com, Office Phone:+40 251 543 739.

Alexandru MARGINE, Associate Professor, PhD, University of Craiova, Faculty of Mechanics, Calea Bucuresti, street, 107, Craiova, Romania, alexandru.margine@gmail.com, Office Phone:+40 251 543 739.

Nicolae DUMITRU, Professor, PhD, University of Craiova, Faculty of Mechanics, Calea Bucuresti, street, 107, Craiova, Romania, nicolae_dtru@yahoo.com, Office Phone:+40 251 543 739.